www.ietdl.org

Published in IET Power Electronics
Received on 22nd February 2013
Revised on 20th December 2013
Accepted on 1st April 2014
doi: 10.1049/iet-pel.2013.0413

ISSN 1755-4535

Single-phase phase locked loop with DC offset and noise rejection for photovoltaic inverters

Slobodan Lubura, Milomir Šoja, Srđan Lale, Marko Ikić

Faculty of Electrical Engineering, University of East Sarajevo, RS, East Sarajevo, Bosnia and Herzegovina
E-mail: slubura@etf.unssa.rs.ba

Abstract: Proper work of grid-connected converters requires an accurate detection of phase angle, frequency and amplitude of grid voltage. Phase locked loops (PLLs) based on synchronous reference frame theory can be used for estimation of these grid parameters. One of the issues that could appear during estimation of grid parameters is appearance of DC offset in measured grid voltage. This DC component (offset) is usually entered in PLL structure via measurement and A/D conversion process. Undesirable induced DC offset could appear as part of the reference sine current of photovoltaic inverters or other grid-connected converters. A lot of standards define allowed PV inverter's DC current injection in the grid. In this study, we propose an improved PLL structure with capability to fully reject DC offset and noise which could appear in measured input grid voltage. The key component of the proposed PLL is two-phase generator with a closed control loop for DC offset and noise rejection. Obtained simulation and experimental results show that the proposed PLL structure can solve important issues of presence of noise and DC offset in measured grid voltage. The proposed PLL structure shows excellent dynamical performances in conditions of fast changes of grid parameters.

Nomenclature

v_{in}	measured input grid voltage with superimposed DC offset
v_α, v_β	two signals in quadrature at the output of two-phase generator
$W_\alpha(s)$, $W_\beta(s)$	transfer functions of band-pass and low-pass filters as components of conventional two-phase generator
s	complex variable
ω	filters' resonant frequency
ω_{est}	estimated grid frequency
k_{i}	integral gain of control loop in the proposed novel two-phase generator for DC offset rejection
$W_{m\alpha}(s)$, $W_{m\beta}(s)$	transfer functions of band-pass filters as components of proposed novel two-phase generator
$V_\alpha(s)$, $V_\beta(s)$	Laplace transformations of signals v_α and v_β
$W_{\text{p}}(s)$	open-loop transfer function of the proposed novel two-phase generator
$D(s)$	characteristic polynomial of the transfer functions of band-pass filters $W_{m\alpha}(s)$ and $W_{m\beta}(s)$
A_i	magnitudes of filters' responses in time domain
τ_1, τ_2	time constants of filters' responses in time domain
$-\zeta\omega_n \pm \text{j}\omega_n\sqrt{1-\zeta^2}$	complex conjugate roots of characteristic polynomial $D(s)$
ζ	damping factor
ω_n	natural frequency
ω_1	imaginary part of complex conjugate roots of characteristic polynomial $D(s)$
a	real root of characteristic polynomial $D(s)$
k_{iopt}	optimal value of integral gain in control loop for DC offset rejection
T_{s}	fundamental sampling time
i_{ref}	reference current of PV inverter
v_{out}	generated reference pure sine signal at the output of PLL structure

1 Introduction

For proper operation and control of various grid-connected converters, such as photovoltaic (PV) inverters, pulse width modulation rectifiers, uninterrupted power supplies (UPSs), distributed power systems and other, it is very important to have information about phase angle, frequency and amplitude of grid voltage. For estimation of mentioned grid parameters are commonly used different phase locked loop (PLL) structures [1–5]. In other words, PLL is a key component of control structure in those converters and has great influence on the power quality, stability and reliability of whole power conversion system. Regardless of the type, each PLL structure should have possibility to reject

© The Institution of Engineering and Technology 2014

17554543, 2014, 9, Downloaded from https://ietresearch.onlinelibrary.wiley.com/doi/10.1049/iet-pel.2013.0413 by Bosnia and Herzegovina Hinari NPL, Wiley Online Library on [07/12/2022]. See the Terms and Conditions (https://onlinelibrary.wiley.com/terms-and-conditions) on Wiley Online Library for rules of use; OA articles are governed by the applicable Creative Commons License

disturbances, such as injected harmonics, frequency variations and phase shifts in the grid voltage etc.

Special attention should be paid to appearance of the DC offset in measured grid voltage during estimation process of the grid parameters. In [4] is shown that estimation errors of the grid parameters which appear because of the induced DC offset have fundamental harmonic component which makes estimation process impossible.

In general, the grid interface circuit should perform three tasks: voltage sensing, filtering and A/D conversion. The non-linearity of voltage sensors, A/D conversion process and the thermal drift of analogue components may cause the existence of DC offset in measured grid voltage, even if the grid interface circuit is well designed.

The introduced DC offset inevitably appears as undesirable part of the reference sine signal on the output of the PLL structure. This reference sine signal is usually used for forming reference current in PV or other grid-connected converters. A lot of standards, such as: IEEE 1547-200 [6], EN61000-3-2 [7] and IEC 61727 [8], define maximum allowed DC current injection in grid caused by PV or other grid-connected converters. Induced DC offset in measured grid voltage could be removed using different methods.

One simple method is using a band-pass filter at the output of grid voltage sensing circuit before entering in a control structure of the grid-connected converters in general. Adding band-pass filter in order to reject induced DC offset could degrade the dynamic performances of overall control structure, because it would be appear in serial connection with other components of control structure. In addition, as has been stated in [9], the addition of this filter could degrade the dynamic performances of PLL structure, which is unacceptable.

Therefore it would be useful that a PLL structure by itself as a part of the control structure in grid-connected converters has capability to reject this DC offset or limit it to maximum allowed value according to the mentioned standards, without adding any external filters.

The single-phase PLL structure based on synchronous reference frame (SRF) theory (PLL-SRF) is widely used [3, 5, 9, 10, 16]. The most important part of the PLL-SRF structure is two-phase generator which should accurately produce two quadrature signals (phase-shifted for $\pi/2$) from single-phase input grid voltage, regardless of the grid disturbances. If any of the grid disturbances caused that the phase difference between signals at the output of two-phase generator is not exactly $\pi/2$, the error in estimation of the grid parameters would appear later. This generator based on inverse Park's transformation is described in [3, 11]. These quadrature signals can also be generated using Hilbert transformer [12].

One method for effective DC offset rejection based on a PLL-SRF technique is proposed in [9]. The rejection of DC offset is performed by inserting a low-pass filter in the structure of the two-phase generator as part of the PLL, but there is no trace of its design. In [10] is proposed PLL-SRF structure with separate part for DC offset rejection consisting of two parts. The first part is integrator for estimation of DC offset error from the synchronous d-axis voltage and the second one is proportional–integral (PI) controller for removing DC offset error. The presented method is more complicated for realisation than the method presented in this paper. In addition, there is no evidence how parameters of the PI controller are chosen.

In [13] we proposed a single-phase PLL-SRF structure with novel two-phase generator which has capability to fully reject induced DC offset and noise. Our basic idea is modification of two-phase generator (1) and (2) and addition of the simple control loop in its structure in order to simultaneously make necessary phase shift and reject induced DC component and noise without adding any additional external filter. Obtained simulation results confirmed suggested idea for rejecting induced DC offset and noise in measured grid voltage. In addition, simulation results confirmed robustness of the proposed two-phase generator with regard to the fast changes of the grid parameters. The proposed generator also possesses excellent grid voltage noise attenuation performance. In [14] we have gone one step further and besides some frequency and stability analysis we have presented experimental verification of the proposed PLL-SRF structure with novel two-phase generator for DC offset and noise rejection.

Besides the main contributions of mentioned published conference papers, this paper covers many points including comprehensive analysis of frequency, stability and response behaviour of the proposed novel two-phase generator as part of PLL-SRF structure. A rigorous optimisation procedure for proper selection of control parameters of novel two-phase generator is also described in detail.

The suggested PLL-SRF structure with a novel two-phase generator can be used for both, grid-connected systems (e.g. PV and wind turbines) and power condition equipment (e.g. UPS and active filters) which rely on PLL-based synchronisation.

This paper is organised as follows. Section 2 describes the PLL-SRF structure with the proposed novel two-phase generator. Section 3 includes derivation of transfer functions and also stability and response analysis of novel two-phase generator. In Section 4 are provided corresponding simulation results. Experimental verification of the proposed PLL-SRF structure with novel two-phase generator is given in Section 5. Section 6 is the conclusion.

2 Novel two-phase generator with DC offset and noise rejection

The single-phase PLL-SRF structure frequently used in grid-connected converters is shown in Fig. 1.

The key component of single-phase PLL-SRF structure is two-phase generator which produces two signals in quadrature v_α and v_β from single-phase grid voltage which is usually distorted. Typically, it consists of second-order filters described in [2, 5, 13, 15]. Transfer functions of these filters, in continuous time domain are given by

$$W_\alpha(s) = \frac{\omega s}{s^2 + \omega s + \omega^2} \tag{1}$$

$$W_\beta(s) = \frac{\omega^2}{s^2 + \omega s + \omega^2} \tag{2}$$

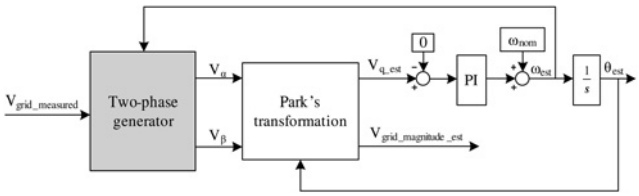

Fig. 1 *Block diagram of single-phase PLL-SRF structure*

© The Institution of Engineering and Technology 2014

17554543, 2014, 9, Downloaded from https://ietresearch.onlinelibrary.wiley.com/doi/10.1049/iet-pel.2013.0413 by Bosnia and Herzegovina Hinari NPL, Wiley Online Library on [07/12/2022]. See the Terms and Conditions (https://onlinelibrary.wiley.com/terms-and-conditions) on Wiley Online Library for rules of use; OA articles are governed by the applicable Creative Commons License

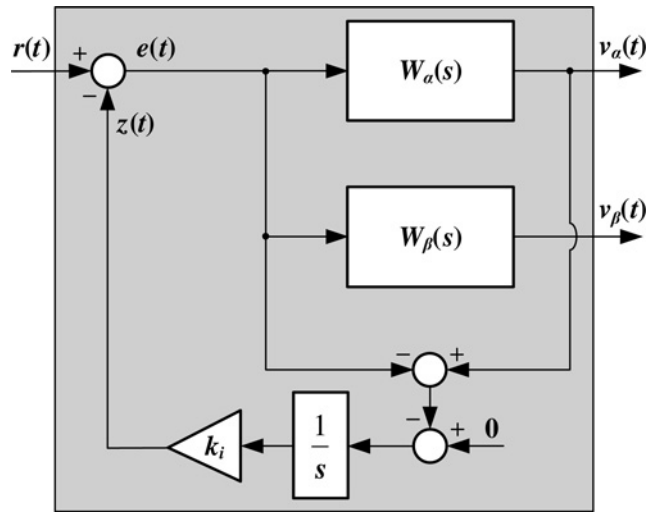

Fig. 2 *Novel two-phase generator with simple closed control loop for DC offset rejection*

Filter $W_\alpha(s)$ is band-pass and $W_\beta(s)$ is low-pass filter, so both filters can successfully attenuate only high-frequency noise and cannot reject induced DC offset if it appears in measured grid voltage. This is the main drawback of two-phase generator and this fact has been shown in [4]. In addition, described two-phase generators (1) and (2) will work properly only if the ω_{est} is matched with the frequency ω. Therefore it is necessary to make adjustment of filters' resonant frequency, which is achieved through the feedback within PLL structure (resonant filters' frequency ω is actually estimated grid frequency ω_{est}).

Induced DC offset in measured grid voltage, as it has been proved in [4], will cause the undesired ripple in estimated values of grid voltage amplitude and frequency. Magnitude of the induced ripple depends on the percentage of DC offset value and it also has fundamental grid frequency.

Hence, the existence of DC offset in measured grid voltage makes the estimation process of the grid parameters practically impossible. A new method for eliminating induced DC offset, which is based on a simple closed control loop with pure integral action as part of two-phase generator, is presented in this paper. Block diagram of this novel two-phase generator is shown in Fig. 2.

Suppose that measured input grid voltage $r(t)$ contains certain DC offset. Estimated value of the DC offset at the control loop output will be obtained and would be further subtracted from input voltage which contains superimposed DC offset, if it exists. The key parameter of the proposed control loop is integral gain k_i. The value of k_i determines the dynamics of the system's transient response. This value has main influence on speed of eliminating the estimation errors caused by induced DC offset in measured grid voltage.

The next section of this paper gives more detailed analysis of the proposed novel two-phase generator with better insight into influence of parameter k_i on overall system response.

3 Transfer function, stability and response analysis of novel two-phase generator

3.1 Transfer function analysis

Transfer functions of new filters that make novel two-phase generator can be derived in following steps, according to Fig. 2

$$\begin{aligned} V_\alpha(s) &= W_\alpha(s)E(s) = W_\alpha(s)(R(s) - Z(s)) \\ &= W_\alpha(s)R(s) - W_\alpha(s)Z(s) \\ V_\beta(s) &= W_\beta(s)E(s) = W_\beta(s)(R(s) - Z(s)) \\ &= W_\beta(s)R(s) - W_\beta(s)Z(s) \end{aligned} \tag{3}$$

where $V_\alpha(s)$, $V_\beta(s)$, $R(s)$, $Z(s)$ and $E(s)$ are Laplace transformations of signals $v_\alpha(t)$, $v_\beta(t)$, $r(t)$, $z(t)$ and $e(t)$, respectively

$$\begin{aligned} Z(s) &= \frac{k_i}{s}\left[0 - \left(V_\alpha(s) - R(s) + Z(s)\right)\right] \\ &= \frac{k_i}{s}\left[-V_\alpha(s) + R(s) - Z(s)\right] \\ &= -\frac{k_i}{s}V_\alpha(s) + \frac{k_i}{s}R(s) - \frac{k_i}{s}Z(s) \Rightarrow \\ Z(s) &= \frac{k_i}{s+k_i}R(s) - \frac{k_i}{s+k_i}V_\alpha \end{aligned} \tag{4}$$

Replacing $Z(s)$ from (4) in (3) and after simplification we obtain

$$\frac{V_\alpha(s)}{R(s)} = W_{m\alpha}(s) = \frac{W_\alpha(s)s}{s + k_i\left(1 - W_\alpha(s)\right)} \tag{5}$$

Replacing $W_\alpha(s)$ from (1) in (5) we obtain

$$\begin{aligned} W_{m\alpha}(s) &= \frac{\left(\omega s^2/\left(s^2 + \omega s + \omega^2\right)\right)}{s + k_i\left(\left(s^2 + \omega^2\right)/\left(s^2 + \omega s + \omega^2\right)\right)} \\ &= \frac{\omega s^2}{s^3 + (\omega + k_i)s^2 + \omega^2 s + k_i\omega^2} \end{aligned} \tag{6}$$

$$\begin{aligned} V_\beta(s) &= W_\beta(s)E(s) = W_\beta(s)\frac{V_\alpha(s)}{W_\alpha(s)} \\ &= \frac{W_\beta(s)}{W_\alpha(s)}W_{m\alpha}(s)R(s) \Rightarrow W_{m\beta}(s) \\ &= \frac{V_\beta(s)}{R(s)} = \frac{W_\beta(s)}{W_\alpha(s)}W_{m\alpha}(s) \end{aligned} \tag{7}$$

Replacing (1), (2) and (6) in (7) we obtain

$$\begin{aligned} W_{m\beta}(s) &= \frac{\left(\omega^2/\left(s^2 + \omega s + \omega^2\right)\right)}{\left(\omega s/\left(s^2 + \omega s + \omega^2\right)\right)}\frac{\omega s^2}{s^3 + (\omega + k_i)s^2 + \omega^2 s + k_i\omega^2} \\ &= \frac{\omega^2 s}{s^3 + (\omega + k_i)s^2 + \omega^2 s + k_i\omega^2} \end{aligned} \tag{8}$$

Note that both filters $W_{m\alpha}(s)$ and $W_{m\beta}(s)$ are band-pass and have the identical denominators, but they have different numerators. The filter $W_{m\alpha}(s)$ has ωs^2, but the filter $W_{m\beta}(s)$ has $\omega^2 s$ term in numerator. This difference is the key for generating the phase difference of $\pi/2$ between the voltages $v_\alpha(t)$ and $v_\beta(t)$ at the output of two-phase generator. Let us replace $s = j\omega_{est}$ in both of filters $W_{m\alpha}$ and $W_{m\beta}$ and it is easy to conclude that the filter $W_{m\alpha}$ entries the zero phase delay, whereas on the other side the filter $W_{m\beta}$ entries the

© The Institution of Engineering and Technology 2014

doi: 10.1049/iet-pel.2013.0413

17554543, 2014, 9, Downloaded from https://ietresearch.onlinelibrary.wiley.com/doi/10.1049/iet-pel.2013.0413 by Bosnia and Herzegovina Hinari NPL, Wiley Online Library on [07/12/2022]. See the Terms and Conditions (https://onlinelibrary.wiley.com/terms-and-conditions) on Wiley Online Library for rules of use; OA articles are governed by the applicable Creative Commons License

$\pi/2$ phase delay regarding to the input measured grid voltage $r(t)$. As band-pass type these filters do not pass both induced DC offset and high-frequency noise if they exist in measured grid voltage. In the previous structure of the two-phase generator (1) and (2) this was not the case, as it was previously discussed.

Stated assertion that the proposed novel two-phase generator does not pass induced DC offset becomes easy to prove using the final value theorem in Laplace domain.

For example, input measured grid voltage can be expressed as: $r(t) = v_{\text{in}}(t) = v_{\text{in0}}(t) + C$, where $v_{\text{in0}}(t) = V_{\text{in}}\sin(\omega t)$ is pure sine measured signal without DC offset and C is induced DC offset value. Laplace transformations of voltages v_α and v_β are given by

$$V_\alpha(s) = W_{m\alpha}(s)V_{\text{in0}}(s) + W_{m\alpha}(s)\frac{C}{s} \tag{9}$$

$$V_\beta(s) = W_{m\beta}(s)V_{\text{in0}}(s) + W_{m\beta}(s)\frac{C}{s} \tag{10}$$

Using final value theorem: $\lim_{t\to\infty} f(t) = \lim_{s\to 0} sF(s)$, where $F(s) = \mathcal{L}\{f(t)\}$, components of voltages v_α and v_β caused by DC offset C vanish in stationary state

$$\begin{aligned}\lim_{s\to 0}\left(sW_{m\alpha}(s)\frac{C}{s}\right) &= \lim_{s\to 0}\left(W_{m\alpha}(s)C\right)\\ &= \lim_{s\to 0}\left(\frac{\omega s^2 C}{s^3 + (\omega + k_{\text{i}})s^2 + \omega^2 s + k_{\text{i}}\omega^2}\right) = 0\end{aligned} \tag{11}$$

$$\begin{aligned}\lim_{s\to 0}\left(sW_{m\beta}(s)\frac{C}{s}\right) &= \lim_{s\to 0}\left(W_{m\beta}(s)C\right)\\ &= \lim_{s\to 0}\left(\frac{\omega^2 sC}{s^3 + (\omega + k_{\text{i}})s^2 + \omega^2 s + k_{\text{i}}\omega^2}\right) = 0\end{aligned} \tag{12}$$

From (11) and (12) is obvious that the proposed two-phase generator could successfully eliminate induced DC offset if it appeared in measured grid voltage.

3.2 Stability analysis

From (6) transfer function $W_{m\alpha}(s)$ can be written as

$$\begin{aligned}W_{m\alpha}(s) &= \frac{\left(\omega s/\left(s^2 + \omega s + \omega^2\right)\right)}{1 + \underbrace{(k_{\text{i}}/s)\left(\left(s^2 + \omega^2\right)/\left(s^2 + \omega s + \omega^2\right)\right)}_{W_{\text{p}}(s)}}\\ &= \frac{W_\alpha(s)}{1 + W_{\text{p}}(s)}\end{aligned} \tag{13}$$

where $W_{\text{p}}(s)$ is open-loop transfer function of the proposed novel two-phase generator.

The same procedure can be followed for transfer function $W_{m\beta}(s)$

$$\begin{aligned}W_{m\beta}(s) &= \frac{\left(\omega^2/\left(s^2 + \omega s + \omega^2\right)\right)}{1 + \underbrace{(k_{\text{i}}/s)\left(\left(s^2 + \omega^2\right)/\left(s^2 + \omega s + \omega^2\right)\right)}_{W_{\text{p}}(s)}}\\ &= \frac{W_\beta(s)}{1 + W_{\text{p}}(s)}\end{aligned} \tag{14}$$

Thus, the open-loop transfer function $W_{\text{p}}(s)$ is equal to

$$W_{\text{p}}(s) = \frac{k_{\text{i}}}{s}\left(\frac{s^2 + \omega^2}{s^2 + \omega s + \omega^2}\right) \tag{15}$$

The root locus of transfer function $W_{\text{p}}(s)$ is given in Fig. 3.

It is obvious from the presented root locus that the proposed novel two-phase generator is stable for every positive gain value k_{i}. However, the value of gain k_{i} has influence on system's dynamics because it determines the position of roots of characteristic polynomial $D(s) = 1 + W_{\text{p}}(s) = s^3 + (\omega + k_{\text{i}})s^2 + \omega^2 s + k_{\text{i}}\omega^2$ in complex s-plane. When gain k_{i} increases, the real part of complex conjugate roots of $D(s)$ increases and approaches the imaginary axis, whereas the real root of $D(s)$ decreases. When gain k_{i} decreases, the real part of complex conjugate roots of $D(s)$ decreases, whereas the real root of $D(s)$ increases and approaches the imaginary axis. Thus, there is a contradiction when choosing a proper value of gain k_{i} because the real root and real parts of complex conjugate roots directly determine time constants of response of two-phase generator. Therefore the optimisation process for selection of gain k_{i} must be performed.

3.3 Response analysis

Supposing that measured input grid voltage contains DC offset and can be expressed as: $v_{\text{in}}(t) = V_{\text{in}}\cos(\omega t) + C$. After performing inverse Laplace transformation of (9) and (10) follows that voltages v_α and v_β are equal to

$$\begin{aligned}v_\alpha(t) = V_{\text{in}}\cos(\omega t) - A\mathrm{e}^{-t/\tau_1} - A_2\mathrm{e}^{-t/\tau_2}\cos(\omega_1 t)\\ + A_3\mathrm{e}^{-t/\tau_2}\sin(\omega_1 t)\end{aligned} \tag{16}$$

$$\begin{aligned}v_\beta(t) = V_{\text{in}}\sin(\omega t) + A_4\mathrm{e}^{-t/\tau_1} - A_5\mathrm{e}^{-t/\tau_2}\\ \times\cos(\omega_1 t) - A_6\mathrm{e}^{-t/\tau_2}\sin(\omega_1 t)\end{aligned} \tag{17}$$

Obviously, after transition of several time constants τ_1 and τ_2, voltages $v_\alpha(t) = V_{\text{in}}\cos(\omega t)$ and $v_\beta(t) = V_{\text{in}}\sin(\omega t)$ at the output of two-phase generator are phase-shifted for $\pi/2$. From (6) and (8) is clear that integral gain k_{i} determines position of poles of $W_{m\alpha}(s)$ and $W_{m\beta}(s)$ in s-plane and therefore the gain k_{i} actually determines the values of time constants τ_1 and τ_2, amplitudes A_i, $i = 1, 2, \ldots, 6$ and frequency ω_1 in time domain, which affects the response of two-phase generator in transient process.

If we denote the real root and complex conjugate roots of characteristic polynomial $D(s)$ as $-a$ $(a > 0)$ and $-\zeta\omega_n \pm \mathrm{j}\underbrace{\omega_n\sqrt{1-\zeta^2}}_{\omega_1} = -\zeta\omega_n \pm \mathrm{j}\omega_1$, respectively, where ζ $(0 < \zeta < 1)$ is damping factor and ω_n is natural frequency, the following applies

$$\begin{aligned}s^3 + (\omega + k_{\text{i}})s^2 + \omega^2 s + k_{\text{i}}\omega^2 &= (s + a)(s^2 + 2\zeta\omega_n s + \omega_n^2)\\ &= s^3 + (a + 2\zeta\omega_n)s^2 + (\omega_n^2 + 2\zeta\omega_n a)s + a\omega_n^2\end{aligned} \tag{18}$$

© The Institution of Engineering and Technology 2014

17554543, 2014, 9, Downloaded from https://ietresearch.onlinelibrary.wiley.com/doi/10.1049/iet-pel.2013.0413 by Bosnia and Herzegovina Hinari NPL, Wiley Online Library on [07/12/2022]. See the Terms and Conditions (https://onlinelibrary.wiley.com/terms-and-conditions) on Wiley Online Library for rules of use; OA articles are governed by the applicable Creative Commons License

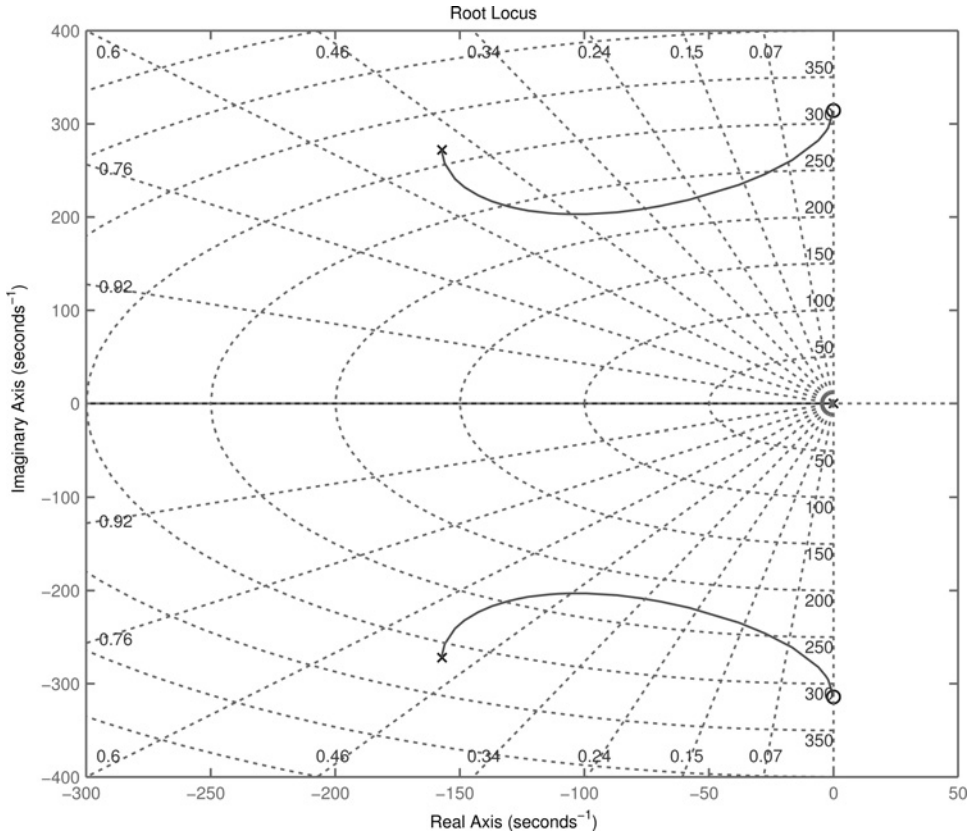

Fig. 3 *Root locus of transfer function $W_p(s)$*

From (18) it follows

$$\omega + k_{\mathrm{i}} = a + 2\zeta\omega_n \tag{19}$$

$$\omega^2 = \omega_n^2 + 2\zeta\omega_n a \tag{20}$$

$$k_{\mathrm{i}}\omega^2 = a\omega_n^2 \tag{21}$$

The expressions of a, ζ and ω_n in terms of the gain k_{i} are given in (19)–(21). Thus, time constants $\tau_1 = 1/a$, $\tau_2 = 1/\zeta\omega_n$ and frequency ω_1 from (16) and (17) are determined by gain k_{i}.

The optimal value of gain k_{i} can be determined from condition of equality of real root $(-a)$ and real part of complex conjugate roots $(-\zeta\omega_n)$. Using $a = \zeta\omega_n$ in (19)–(21) we obtain

$$\omega + k_{\mathrm{i}} = 3a \tag{22}$$

$$\omega^2(a - k_{\mathrm{i}}) = 2a^3 \tag{23}$$

Using $\omega = 2\pi f$, $f = 50$ Hz, and solving (22) and (23) for a and k_{i}, we obtain

$$a = 133.1576 \tag{24}$$

$$k_{\mathrm{i}} = 85.3135 = k_{\mathrm{iopt}} \tag{25}$$

The obtained value of gain k_{i} in (25) is optimal.

Step responses (signals v_α and v_β) of the transfer functions $W_{m\alpha}(s)$ and $W_{m\beta}(s)$ for three different values of gain k_{i} are presented in Fig. 4.

If we compare step response (Fig. 6*b*) in [9] of the closed-loop transfer function $H_q(s)$ given by (3) in [9], which is the same transfer function as $W_\beta(s)$ in (2) from this paper, with step response of the closed-loop transfer function $W_{m\beta}(s)$ from (8) (Fig. 4, solid black line), it is obvious that we obtained better step response for our proposed DC offset rejection method than the one provided in [9].

4 Simulation results of proposed PLL structure

If proposed PLL structure is used as part of control structure of grid tied PV inverters in order to perform islanding detection or abnormal grid conditions (trip time) for example, its behaviour in steady state and its transient response must be tested according to requirements of standards such as IEEE 1547 [6] and IEC 61727 [8]. Performances of the proposed PLL structure were tested through simulations in MATLAB/SIMULINK. The behaviour of the proposed PLL structure in steady state was first tested. The sine input voltage $v_{\mathrm{in}}(t) = 230\sqrt{2}\sin(\omega t) + 100$ V with large, ~30%, DC offset, was entered to the two-phase generator. Two cases were analysed. The first one is without closed loop for DC offset rejection, whereas the second one includes proposed control loop. Integral gain k_{i} had fixed value and equal to optimal value k_{iopt} from (25). The simulation results are shown in Fig. 5.

In first case (no control loop for DC offset rejection) it is obvious that estimated grid voltage amplitude and frequency in steady state contain fundamental ripple component (50 Hz) and it is not possible to accurately determine these parameters. In second case (included control loop) induced DC offset is completely removed and there is no ripple in estimated parameters.

To test transient response of the proposed PLL structure and determine the influence of parameter k_{i} on estimation

© The Institution of Engineering and Technology 2014

doi: 10.1049/iet-pel.2013.0413

17554543, 2014, 9, Downloaded from https://ietresearch.onlinelibrary.wiley.com/doi/10.1049/iet-pel.2013.0413 by Bosnia and Herzegovina Hinari NPL, Wiley Online Library on [07/12/2022]. See the Terms and Conditions (https://onlinelibrary.wiley.com/terms-and-conditions) on Wiley Online Library for rules of use; OA articles are governed by the applicable Creative Commons License

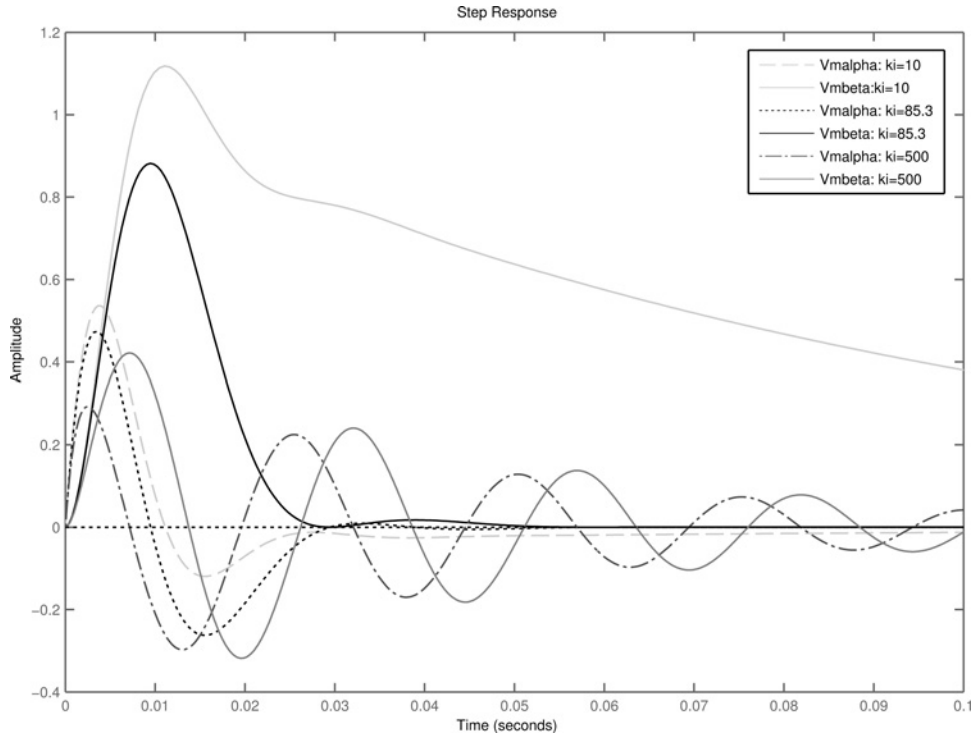

Fig. 4 *Step responses of transfer functions $W_{m\alpha}(s)$ (dashed line) and $W_{m\beta}(s)$ (solid line) for different values of k_i*

process, simulations were performed for three different values of gain k_i:1, k_{iopt} and 500. The results are shown in Fig. 6.

At the point in time of 1 s the grid amplitude was suddenly changed from $310\sqrt{2}$ to $115\sqrt{2}$ V and reversed at the point in time of 2.5 s. In the same points in time, grid frequency was suddenly changed from 51 to 49 Hz and vice versa. The value of induced DC offset in grid voltage was 100 V in both cases. The best response was obtained for $k_i = k_{iopt}$, whereas for the

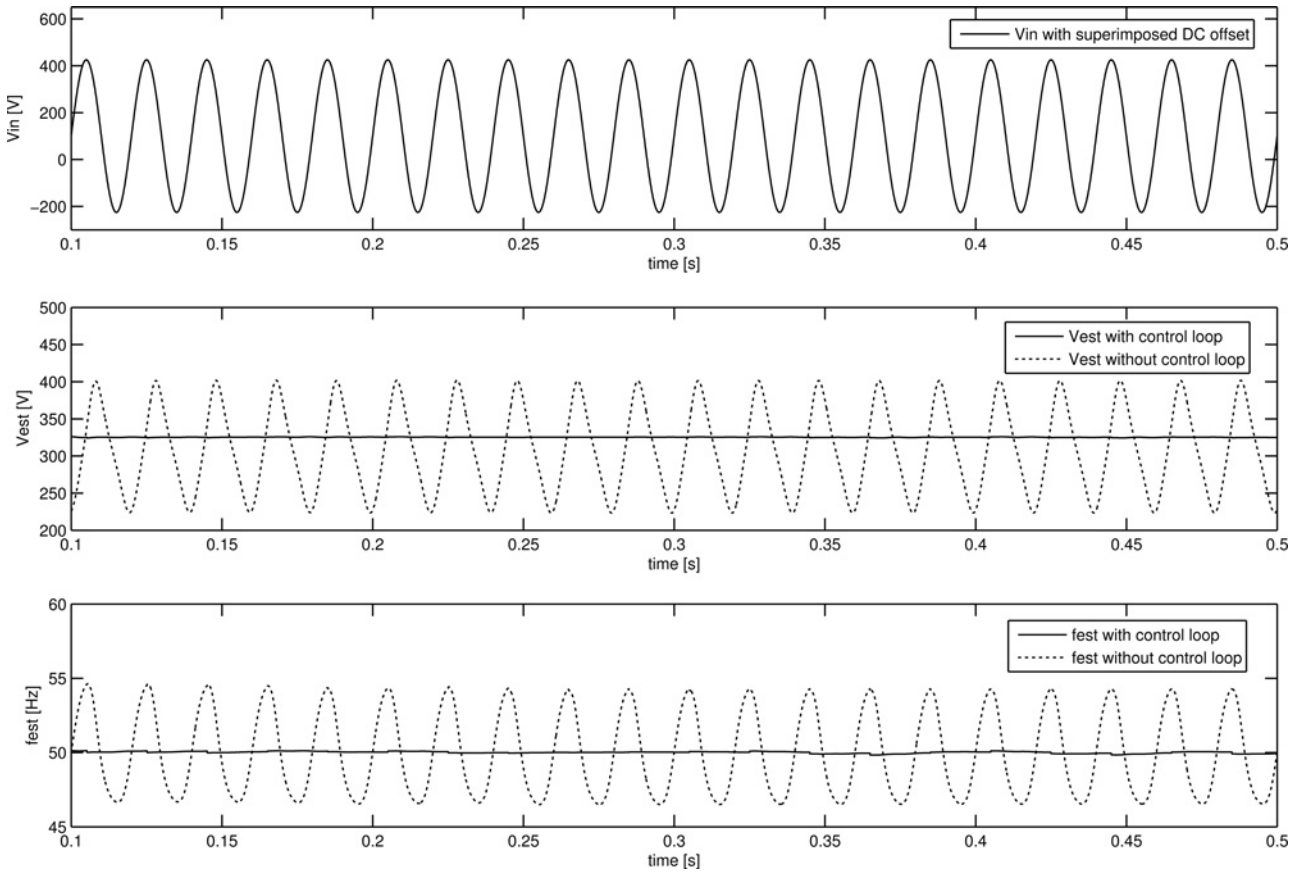

Fig. 5 *Estimated grid amplitude and frequency in steady state: without (dotted line) and with control loop for DC offset rejection (solid line)*

© The Institution of Engineering and Technology 2014

17554543, 2014, 9, Downloaded from https://ietresearch.onlinelibrary.wiley.com/doi/10.1049/iet-pel.2013.0413 by Bosnia and Herzegovina Hinari NPL, Wiley Online Library on [07/12/2022]. See the Terms and Conditions (https://onlinelibrary.wiley.com/terms-and-conditions) on Wiley Online Library for rules of use; OA articles are governed by the applicable Creative Commons License

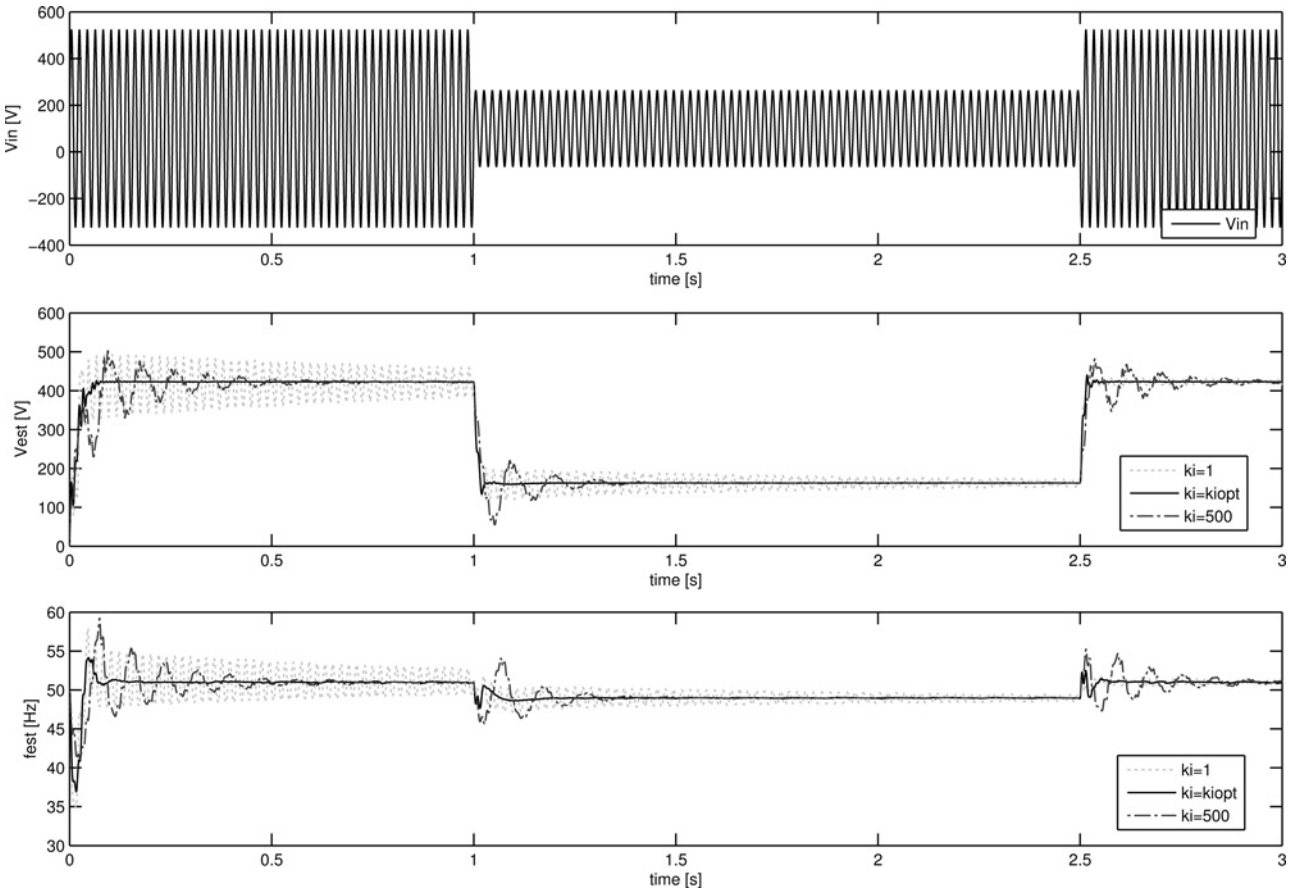

Fig. 6 *Transient response of proposed PLL structure: estimated amplitude (top) and frequency (bottom) of grid voltage for $k_i = 1$, k_{iopt} and 500*

$k_i = 1$ and 500 oscillations appeared. The worst case was noted when $k_i = 1$.

For lower value of gain ($k_i = 1$), damped oscillations in estimated grid voltage amplitude and frequency appear (Fig. 6) and estimation process is not too fast. These oscillations contain fundamental ripple component (51 or 49 Hz), because this small value of gain k_i very slowly rejects the introduced DC offset in measured input voltage, as it is pointed in [4]. When high value of gain ($k_i = 500$) is used, in transient response large oscillations also appear with frequency being depend on the roots of characteristic polynomial $D(s)$.

From Fig. 6 it is easy to conclude that for $k_i = k_{iopt}$ transient response is finished for ~0.1 s and estimated parameters have taken steady-state values. This transient response time of the proposed PLL structure is lower than given trip time of PV grid tied inverters defined in IEC 61727 standard (response for abnormal grid voltage $50\%V_{nominal} < V < 135\%V_{nominal}$ – 2 s and response on over/under frequency 49 Hz $< f <$ 51 Hz – 0.2 s) and the proposed PLL structure can be successfully used for detection abnormal grid conditions.

5 Experimental results of proposed PLL structure

In addition, performances of the proposed PLL structure were verified through several experiments in real time. The developed experimental platform (Fig. 7*a*) has three components:

- grid interface board – galvanic isolation, filtering and scaling of measured grid voltage according to requirements of analogue input of multifunctional input/output (I/O) board;
- multifunctional I/O board MF624 – supported from MATLAB 'real-time windows target' (RTWT) toolbox for connecting 'real world' with MATLAB/SIMULINK environment; and
- PC computer with MATLAB/SIMULINK and installed RTWT toolbox – for rapid prototyping and fast development of control structures.

The grid interface board accepts a real grid voltage $v_{in} = 230\sqrt{2}\sin(\omega t)$ V, performs galvanic isolation by isolation transformer, filtering and scaling its value according to requirements of analogue input of I/O board (±10 V). The filtered and scaled signal is further brought to analogue input at I/O board and sampled by 14 bit A/D converter. In MATLAB/SIMULINK environment, it gets accepted via analogue input block as part of RTWT toolbox. All parts of the proposed PLL structure were built in MATLAB/SIMULINK environment as shown in Fig. 7*b*. For real-time operation, fundamental sampling time T_s of 50 μs was chosen.

Since input grid voltage does not necessarily have to possess DC offset in real measurement process, it was necessary to artificially inject DC offset in measured grid voltage in order to evaluate performances of the proposed PLL structure. It was done by summing actual measured grid voltage with a constant value from SIMULINK. In addition, in order to test performances of the proposed PLL structure under noise

© The Institution of Engineering and Technology 2014

doi: 10.1049/iet-pel.2013.0413

17554543, 2014, 9, Downloaded from https://ietresearch.onlinelibrary.wiley.com/doi/10.1049/iet-pel.2013.0413 by Bosnia and Herzegovina Hinari NPL, Wiley Online Library on [07/12/2022]. See the Terms and Conditions (https://onlinelibrary.wiley.com/terms-and-conditions) on Wiley Online Library for rules of use; OA articles are governed by the applicable Creative Commons License

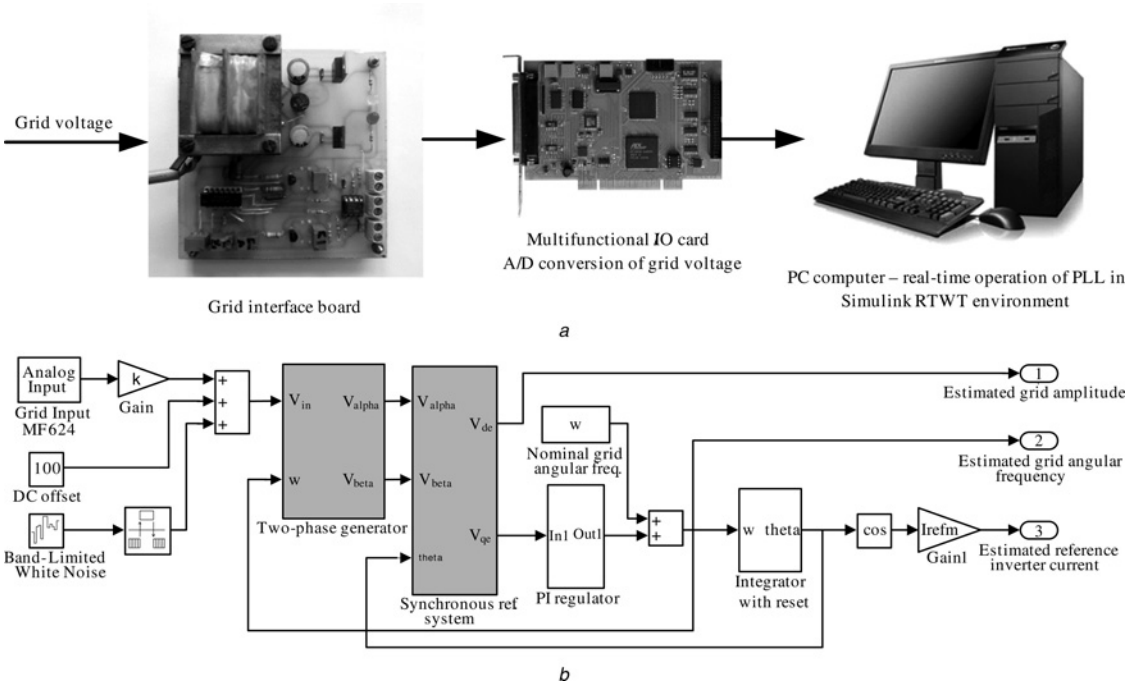

Fig. 7 *Implementation of proposed PLL structure*

a Experimental platform for testing of proposed PLL structure
b Realisation of proposed PLL in SIMULINK (for real-time processing)

conditions, it was possible to add some white noise together with measured grid signal. This was performed by adding band limited white noise generator output from SIMULINK to measured grid voltage with DC offset.

The possibilities of adding noise and DC offset artificially (independently) from SIMULINK to the measured grid voltage makes this experimental platform very powerful for testing performances of PLL.

5.1 Robustness of two-phase generator with regard to added input noise

The nominal value of grid voltage $v_{\text{in}} = 230\sqrt{2}\,\sin(100\pi t)$ V was applied on input of grid interface board. The measured grid voltage was accepted in MATLAB environment and summed with white noise generator at input of two-phase generator, in order to check

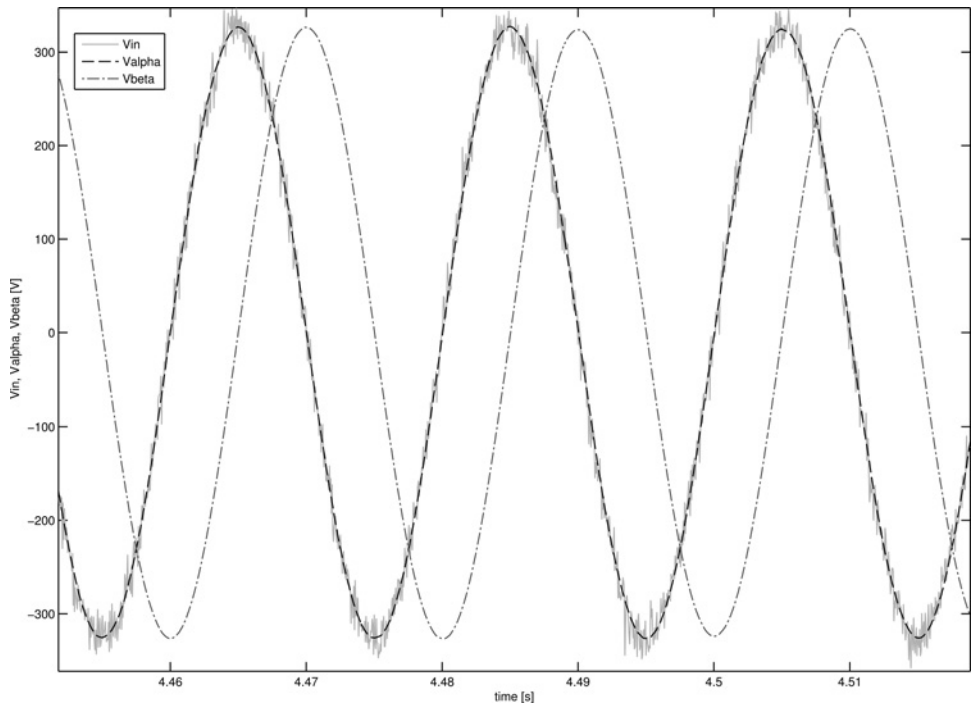

Fig. 8 *Real-time response of two-phase generator on input grid voltage with added noise*

© The Institution of Engineering and Technology 2014

17554543, 2014, 9, Downloaded from https://ietresearch.onlinelibrary.wiley.com/doi/10.1049/iet-pel.2013.0413 by Bosnia and Herzegovina Hinari NPL, Wiley Online Library on [07/12/2022]. See the Terms and Conditions (https://onlinelibrary.wiley.com/terms-and-conditions) on Wiley Online Library for rules of use; OA articles are governed by the applicable Creative Commons License

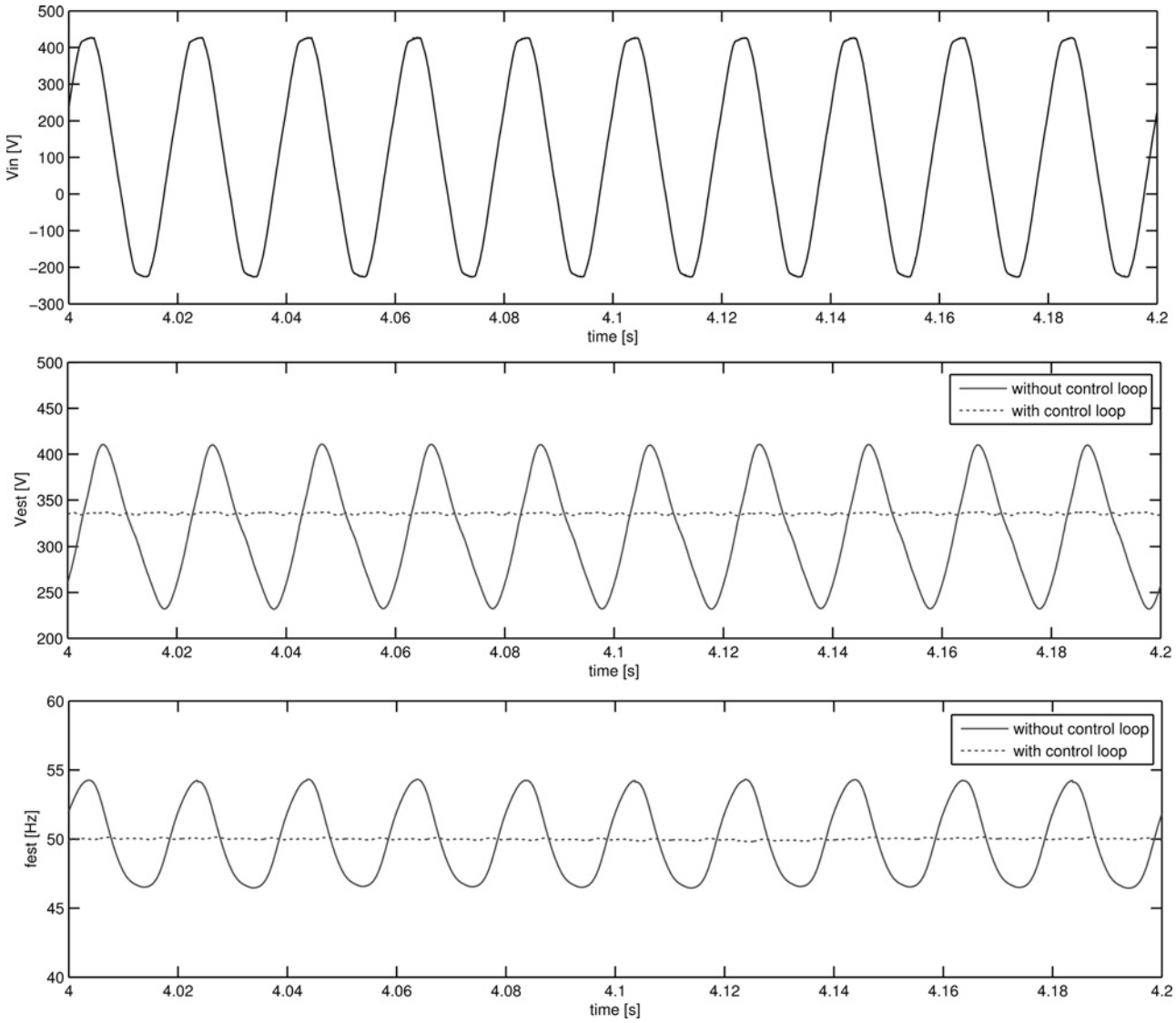

Fig. 9 *Estimated grid parameters in steady state: input grid voltage $v_{in} = 230\sqrt{2}\sin(\omega t) + 100\,V$ with 30% added DC offset (top); grid amplitude (middle) and grid frequency (bottom), without (solid line) and with control loop for DC offset rejection (dotted line)*

its response on input grid voltage with added white noise. The height of the power spectral density of added white noise was 0.0095. Fig. 8 shows response of two-phase generator (v_α and v_β) on input grid voltage with added white noise. It is obvious that the proposed two-phase generator has ability to successfully attenuate induced noise because of existence of the band-pass filters in its structure.

5.2 Estimated grid parameters without/with control loop for DC offset rejection

To test ability of the proposed PLL to reject DC offset in measured grid voltage, DC offset (~30% of magnitude of grid voltage) was artificially added in the measured grid voltage and several experiments were performed. Steady-state analysis was first done. Fig. 9 shows the waveforms of estimated grid parameters: amplitude and frequency, in cases without and with control loop for DC offset rejection.

The value of added DC offset in measured grid voltage is quite large, about 100 V (the same value was used in performed simulations), so applied voltage on the input of the PLL structure can be expressed as: $v_{in} = 230\sqrt{2}\,\sin(\omega t) + 100$ V. It is obvious that added DC offset causes a large ripple component in estimated values of amplitude and frequency of grid voltage (Fig. 9), in case without control loop for DC offset rejection.

When novel two-phase generator with control loop for DC offset rejection was used, a large ripple component in estimated values of grid amplitude and frequency completely vanished in steady state (Fig. 9). The used gain in control loop for DC offset rejection k_i was k_{iopt}. The obtained experimental results are very similar to given corresponding simulation results.

5.3 Response of proposed PLL structure against fast changes of grid parameters

As it is mentioned earlier in this paper, if PLL structure is used in grid tied PV inverters, its transient responses must satisfy mentioned standards. Therefore it was very important to verify robustness of whole PLL structure with regard to fast changes of the grid parameters for different values of gain k_i in real time. For this purpose, two analogue channels of multifunctional I/O card were used. The first one is for measured real grid voltage (interface board). The second one is for function generator that simultaneously mimics: extreme grid conditions [smaller

© The Institution of Engineering and Technology 2014

doi: 10.1049/iet-pel.2013.0413

17554543, 2014, 9, Downloaded from https://ietresearch.onlinelibrary.wiley.com/doi/10.1049/iet-pel.2013.0413 by Bosnia and Herzegovina Hinari NPL, Wiley Online Library on [07/12/2022]. See the Terms and Conditions (https://onlinelibrary.wiley.com/terms-and-conditions) on Wiley Online Library for rules of use; OA articles are governed by the applicable Creative Commons License

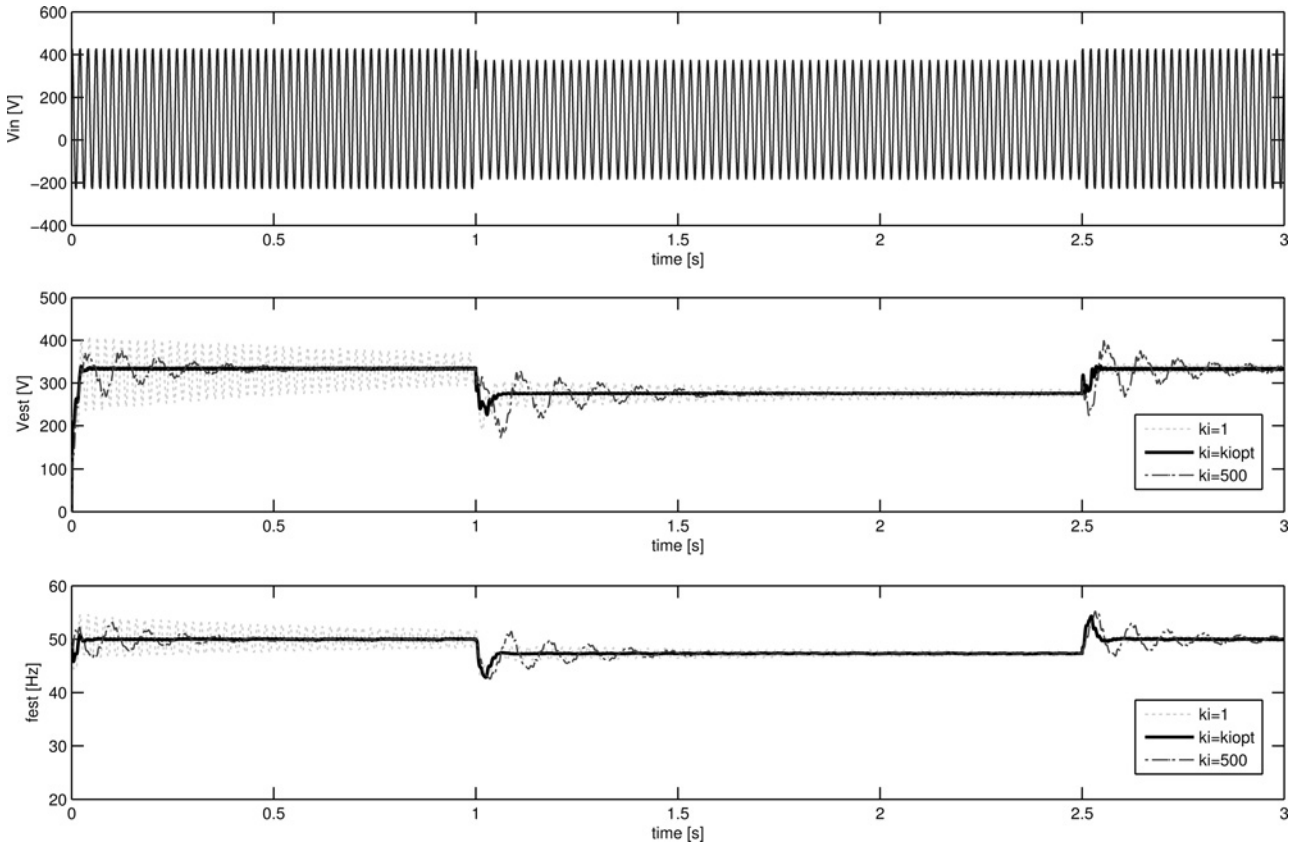

Fig. 10 *Real-time response of proposed PLL structure: estimated grid amplitude and frequency for $k_i = 1$, k_{iopt} and 500*

grid amplitude (280 V) and lower frequency (47 Hz)] and failure in grid interface board such as induced DC offset (roughly 30% of magnitude of grid voltage). Change of grid voltage was done according to standard IEC 61727 for continuous operation of grid tied PV inverters, but frequency change was done in wider range according to requirements of design of PV microinverters on market.

By switching between these sources, it was possible to simultaneously simulate rapid changes of grid parameters (frequency, amplitude or both) under failure in the grid interface board. At the point in time of 1 s, input of two-phase generator was switched from grid to function generator and reversed at the point in time of 2.5 s. Three different values of gain k_i were used (1, $k_{iopt} = 85.3$ and 500).

To obtain consistent experimental results and to more clearly prove the theory analysis, we performed experiments under the same conditions for each value of gain k_i. By using external trigger circuit, we ensured event-related synchronisation which means that instantaneous values of grid voltage and output of function generator were equal in switching points in time for all performed experimental tests.

The experimental results are shown in Fig. 10. When lower value of gain is used ($k_i = 1$), it is obvious that large oscillations in estimated grid voltage amplitude and frequency appear and it is possible to accurately estimate these parameters only after enough time, which is much longer than for higher values of gain k_i. These oscillations contain fundamental ripple component (50 or 47 Hz), as it has been explained and proved with our obtained simulation results. When $k_i = 500$ is used, in transient response large oscillations also appear, but they do not contain fundamental ripple component. Instead the response contains frequency which depends on the roots of characteristic polynomial $D(s)$ as it was mentioned earlier in this paper. In addition, the settling time for this response is much shorter than for the value of gain $k_i = 1$.

From Fig. 10 is obvious that the response of the proposed PLL structure against fast changes of grid parameters is the best when the optimal value of gain $k_i = k_{iopt}$ is used.

Comparing the experimental results from Fig. 10 with the simulation results from Fig. 6, it is obvious that the obtained experimental results are matched with the simulation results and obtained transient response time is lower than given trip time defined in mentioned standards.

5.4 Generating reference sine current for PV grid-connected inverters

The main task of PLL, as part of control structure in grid-connected PV inverters, is generating a sine signal in phase with grid voltage which can be used as reference current $i_{ref} = i_g^* \sin \hat{\theta}_g$ of PV inverter, as shown in Fig. 11.

It is very important that this sine reference current signal does not contain DC offset and higher harmonic components [17–20], as it has been defined according to the mentioned IEEE, EN and IEC standards.

In Fig. 12 is shown waveform of grid voltage with added DC offset $v_{in} = 230\sqrt{2}\sin(\omega t) + 100$ V, supplied on the input of the proposed PLL structure, and also a waveform of generated reference sine signal v_{out} at the output of PLL structure. It is common that reference sine signal at the output of PLL structure is normalised to one, but in Fig. 12 this signal is scaled (gained) by $230\sqrt{2}$ in order to compare it with input grid voltage with induced DC offset. It is obvious that output sine signal does not contain DC offset and other higher harmonic components. This means that this undesired induced DC offset was successfully eliminated by the proposed PLL structure.

© The Institution of Engineering and Technology 2014

17554543, 2014, 9, Downloaded from https://ietresearch.onlinelibrary.wiley.com/doi/10.1049/iet-pel.2013.0413 by Bosnia and Herzegovina Hinari NPL, Wiley Online Library on [07/12/2022]. See the Terms and Conditions (https://onlinelibrary.wiley.com/terms-and-conditions) on Wiley Online Library for rules of use; OA articles are governed by the applicable Creative Commons License

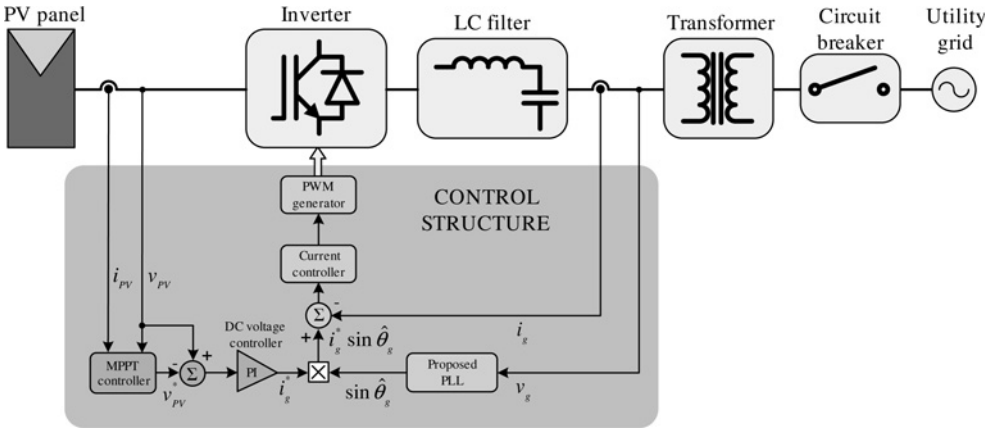

Fig. 11 *Block diagram of grid-connected PV inverter with control structure*

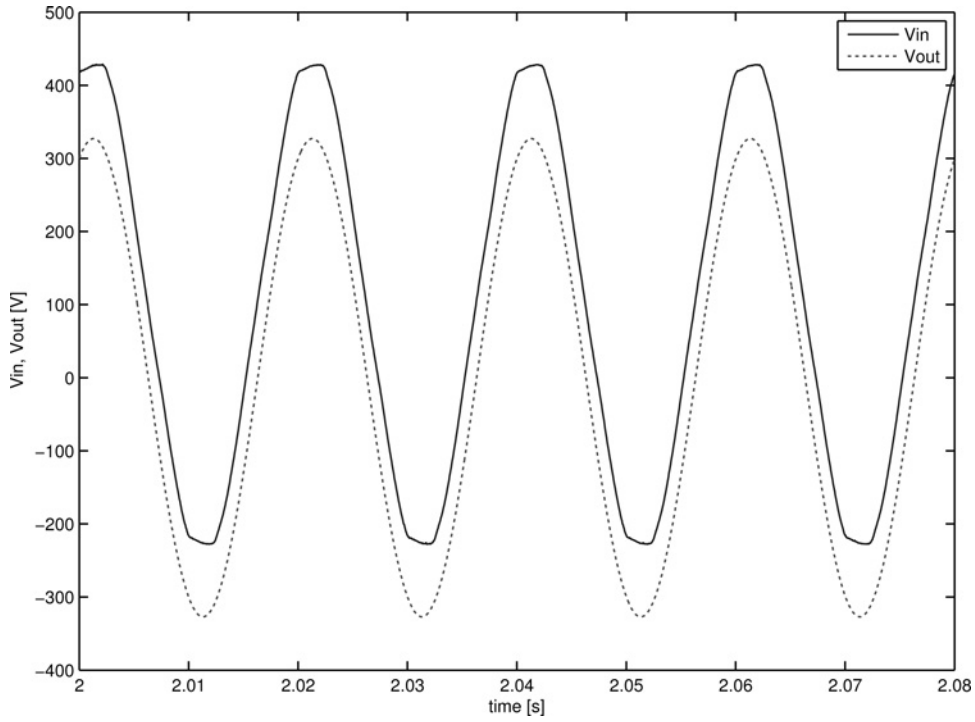

Fig. 12 *Input grid voltage with 30% DC offset and scaled output reference current without DC offset*

Described PLL-SRF structure with novel two-phase generator was designed in continuous time domain, but experimental results were obtained by multifunctional I/O card in real time in SIMULINK RTWT environment. A/D conversion process by self behaves as zero-order hold circuit and converts signal from analogue to digital form. On this way our PLL structure was actually implemented in digital form, where we used double format for data presentation in RTWT SIMULINK environment. It is clear that is not possible to obtain a 'pure' sine signal, but digital staircase sine signal at the output of such realised PLL structure. However, the speed of measuring and processing data (fundamental sampling time $T_s = 50\ \mu s$) in our experimental setup was enough fast to obtain the quite satisfying sine reference signal at the output of the PLL, as shown in Fig. 12.

Applied real-time signal processing is suitable for use for a number of reasons: it allows us to make algorithms in graphical environment, which can be much easier then textual programming; the algorithm can be changed and updated quickly and even during real-time processes; the results (variables, signals and other) can be easy monitored in various ways (scopes, displays, recording values to files etc.). One of the main advantages of RTWT environment is excellent speed of data processing because of used multifunctional I/O card which has very good performances.

6 Conclusion

In this paper was presented PLL-SRF structure with novel two-phase generator for DC offset and noise rejection. Corresponding simulation and experimental results were provided. Obtained results show that the proposed PLL-SRF structure can solve important issues of presence of noise and DC offset in measured grid voltage. In addition, the whole PLL-SRF structure preserves excellent dynamical performances in conditions of fast changes of grid parameters. This PLL-SRF structure could be excellent solution as part of control structure of PV inverters and other grid-connected converters. The further steps should be

© The Institution of Engineering and Technology 2014

17554543, 2014, 9, Downloaded from https://ietresearch.onlinelibrary.wiley.com/doi/10.1049/iet-pel.2013.0413 by Bosnia and Herzegovina Hinari NPL, Wiley Online Library on [07/12/2022]. See the Terms and Conditions (https://onlinelibrary.wiley.com/terms-and-conditions) on Wiley Online Library for rules of use; OA articles are governed by the applicable Creative Commons License

made in two directions. First is improvement of presented PLL-SRF structure to enable it to fully reject low-order harmonics (3rd, 5th, ...) if they exist in measured grid voltage and the second is implementation of the proposed PLL structure to certain digital platforms such as digital signal processor (DSP), field programmable gate array (FPGA) circuits as part of control structure in grid-connected converters.

7 References

1 Kaura, V., Blasko, V.: 'Operation of a phase locked loop system under distorted utility conditions', *IEEE Trans. Ind. Appl.*, 1997, **33**, (1), pp. 58–63, doi: 10.1109/28.567077

2 Yuan, X., Merk, W., Stemmler, H., Allmeling, J.: 'Stationary-frame generalized integrators for current control of active power filters with zero steady-state error for current harmonics of concern under unbalanced and distorted operating conditions', *IEEE Trans. Ind. Appl.*, 2002, **38**, (2), pp. 523–532, doi: 10.1109/28.993175

3 Arruda, L.N., Silva, S.M., Filho, B.J.C.: 'PLL structures for utility connected systems'. 36th IAS Annual Meeting. Conf. Record of the 2001 IEEE Industry Applications Conf., 2001, 30 September 2001–4 October 2001, vol. 4, pp. 2655–2660, doi: 10.1109/IAS.2001.955993

4 Chung, S.-K.: 'Phase-locked loop for grid-connected three-phase power conversion systems'. IEE Proc. Electric Power Applications, May 2000, vol. 147, no. 3, pp. 213–219, doi: 10.1049/ip-epa:20000328

5 Ciobotaru, M., Teodorescu, R., Blaabjerg, F.: 'A new single-phase PLL structure based on second order generalized integrator'. 37th IEEE Power Electronics Specialists Conf., 2006. PESC '06, 18–22 June 2006, pp. 1–6, doi: 10.1109/PESC.2006.1711988

6 IEEE Std 1547-2003: 'IEEE standard for interconnecting distributed resources with electric power systems', 2003, pp. 0_1–16, doi: 10.1109/IEEESTD.2003.94285

7 CENELEC EN 61000-3-2:2000: 'Electromagnetic compatibility (EMC) – part 3-2: limits – limits for harmonic current emissions (equipment input current up to and including 16 A per phase)'

8 IEC 61727-2004: 'Photovoltaic (PV) systems – characteristics of the utility interface'

9 Ciobotaru, M., Teodorescu, R., Agelidis, V.G.: 'Offset rejection for PLL based synchronization in grid-connected converters'. 23rd Annual IEEE Applied Power Electronics Conf. Exposition, 2008. APEC 2008, 24–28 February 2008, pp. 1611–1617, doi: 10.1109/APEC.2008.4522940

10 Hwang, S.-H., Liu, L., Li, H., Kim, J.-M.: 'DC offset error compensation for synchronous reference frame PLL in single-phase grid-connected converters', *IEEE Trans. Power Electron.*, 2012, **27**, (8), pp. 3467–3471, doi: 10.1109/TPEL.2012.2190425

11 Silva, S.M., Lopes, B.M., Filho, B.J.C., Campana, R.P., Bosventura, W. C.: 'Performance evaluation of PLL algorithms for single-phase grid-connected systems'. 39th IAS Annual Meeting. Conf. Record of the 2004 IEEE Industry Applications Conf., 2004, 3–7 October 2004, vol. 4, pp. 2259–2263, doi: 10.1109/IAS.2004.1348790

12 Saitou, M., Matsui, N., Shimizu, T.: 'A control strategy of single-phase active filter using a novel d-q transformation'. 38th IAS Annual Meeting. Conf. Record of the Industry Applications Conf., 2003, 12–16 October 2003, vol. 2, pp. 1222–1227, doi: 10.1109/IAS.2003.1257706

13 Lale, S., Lubura, S., Šoja, M., Ikić, M.: 'Analysis of single-phase PLL with novel two-phase generator for grid-connected converters'. 2011 19th Telecommunications Forum (TELFOR), 22–24 November 2011, pp. 715–718, doi: 10.1109/TELFOR.2011.6143645

14 Lubura, S., Šoja, M., Lale, S., Ikić, M.: 'Experimental verification of single-phase PLL with novel two-phase generator for grid-connected converters'. 201215th International Power Electronics and Motion Control Conf. (EPE/PEMC), 4–6 September 2012, pp. DS3f.1-1–DS3f.1-5, doi: 10.1109/EPEPEMC.2012.6397367

15 Fukuda, S., Yoda, T.: 'A novel current-tracking method for active filters based on a sinusoidal internal model [for PWM invertors]', *IEEE Trans. Ind. Appl.*, 2001, **37**, (3), pp. 888–895, doi: 10.1109/28.924772

16 Dong, D., Boroyevich, D., Mattavelli, P., Cvetkovic, I.: 'A high-performance single-phase phase-locked-loop with fast line-voltage amplitude tracking'. 2011 26th Annual IEEE Applied Power Electronics Conf. and Exposition (APEC), 6-11 March 2011, pp. 1622–1628, doi: 10.1109/APEC.2011.5744812

17 Cho, Y.: 'Observer based online current offset compensation method for single-phase photovoltaic inverter applications', *Electron. Lett.*, 2012, **48**, (23), pp. 1493–1495, doi: 10.1049/el.2012.2760

18 Bowtell, L., Ahfock, A.: 'Direct current offset controller for transformerless single-phase photovoltaic grid-connected inverters', *IET Renew. Power Gener.*, 2010, **4**, (5), pp. 428–437, doi: 10.1049/iet-rpg.2009.0043

19 Berba, F., Atkinson, D., Armstrong, M.: 'A review of minimization of output DC current component methods in single-phase grid-connected inverters PV applications'. 2012 2nd Int. Symp. Environment Friendly Energies and Applications (EFEA), 25–27 June 2012, pp. 296–301, doi: 10.1109/EFEA.2012.6294058

20 Dasgupta, S., Mohan, S.N., Sahoo, S.K., Panda, S.K.: 'Derivation of instantaneous current references for three phase PV inverter connected to grid with active and reactive power flow control'. 2011 IEEE 8th Int. Conf. Power Electronics and ECCE Asia (ICPE & ECCE), 30 May 2011–3 June 2011, pp. 1228–1235, doi: 10.1109/ICPE.2011.594468

© The Institution of Engineering and Technology 2014

17554543, 2014, 9, Downloaded from https://ietresearch.onlinelibrary.wiley.com/doi/10.1049/iet-pel.2013.0413 by Bosnia and Herzegovina Hinari NPL, Wiley Online Library on [07/12/2022]. See the Terms and Conditions (https://onlinelibrary.wiley.com/terms-and-conditions) on Wiley Online Library for rules of use; OA articles are governed by the applicable Creative Commons License